Maximum-Likelihood Estimation of Specific Differential Phase and Attenuation in Rain

V. Santalla del Rio, *Member, IEEE*, Yahia M. M. Antar, *Fellow, IEEE*, and Xavier Fàbregas, *Member, IEEE*

***Abstract*—Precise estimation of propagation parameters in precipitation media is of interest to improve the performance of communications systems and in remote sensing applications. In this paper, we present maximum-likelihood estimators of specific attenuation and specific differential phase in rain. The model used for obtaining the cited estimators assumes coherent propagation, reflection symmetry of the medium, and Gaussian statistics of the scattering matrix measurements. No assumptions about the microphysical properties of the medium are needed. The performance of the estimators is evaluated through simulated data. Results show negligible estimators bias and variances close to Cramer–Rao bounds.**

***Index Terms*—Maximum-likelihood (ML) estimation, propagation parameters, weather radar.**

I. Introduction

ATTENUATION experienced by radiowaves that propagate through a precipitation medium has been studied since the first radar systems became operational. The most recent development of polarimetric radars has also focused attention on cross-polarization effects suffered by waves propagating in a rain medium.

The expansion of communications systems that employ dual polarizations in the same frequency band, and polarimetric weather radar services for remote sensing of precipitation has enforced the study, the characterization, and the modeling of propagation through precipitation media.

Rain effects on wave propagation can basically be considered coherent, at least in the microwave and millimeter-wave regions [1]. Modeling and analysis of rain effects on coherent wave propagation have been addressed by different authors. Of particular interest is the review and comparison of the different coherent models developed by Olsen [2], where attention is focused on the similarities and differences between several general formulations for precipitation media with random scatterer orientations, and the implications of realizing different assumptions and considerations about the microphysical properties of the medium (distribution of sizes, orientations, etc.) on the expressions for the propagation constants. The role of multiple scattering in these formulations is also discussed. It is of interest to point out that all assumptions realized about the distribution of sizes and orientations with the different formulations lead to orthogonal characteristic polarizations. Later, it was proved [3] that this orthogonality is a consequence of the reflection symmetry that rain media usually present. Therefore, orthogonality of characteristic polarizations will be assumed in the rest of the paper.

Estimation of propagation parameters has also been discussed by different authors. To estimate the differential propagation phase shift, several methods based on the analysis of the copolar correlation phase have been proposed. Of importance are those described in [4]–[7]. Estimation of specific and differential attenuation has relied on physical models relating the specific attenuation at orthogonal polarizations with directly measurable quantities, basically the reflectivity, the differential reflectivity, and the specific differential phase [8]–[11]. An interesting review and comparison of these methods can be found in [12].

In this paper, a new approach to propagation parameter estimation based on the maximum-likelihood (ML) statistical theory is considered. ML estimates are usually of interest because they present two important properties.

1) In the limiting case of a large number of samples, and under certain general regularity conditions, they are unbiased.
2) If the estimates are unbiased, they have minimum variance, and this variance achieves the Cramer–Rao bound.

To obtain ML estimators of the differential propagation parameters statistical characterization of the scattering matrix measurements is required. It is generally accepted that scattering matrix measurements from rain are well described by a multivariate complex Gaussian distribution. This distribution is completely defined by the covariance matrix. Section II is devoted to model the polarimetric covariance matrix considering propagation effects. In Section III, statistical characterization of received polarimetric data is briefly reviewed. Then, in Section IV, ML estimates of specific attenuation and specific differential phase are obtained. After, a sensitivity analysis of the calculated ML estimators to different measurement errors and some results based on simulations are presented. Finally some conclusions are made.

II. Propagation Effects on Scattering and Covariance Matrix Elements: Basic Theory

Based on the previous brief review and discussion, propagation effects on the scattering and the covariance matrices will be modeled, assuming coherent propagation through an anisotropic

Manuscript received August 2, 2002; revised June 29, 2003. This work was supported in part by the Spanish Comisión Interministerial de Ciencia y Tecnología under Grant TIC1999-1050-C03-02.

V. Santalla del Rio is with the Department of Teoría de la Señal y Comunicaciones, Universidad de Vigo, 36200 Vigo, Spain (e-mail: vsantall@grp.tsc.uvigo.es).

Y. M. M. Antar is with the Department of Electrical and Computer Engineering., Royal Military College, Kingston, ON K7K 5LO, Canada (e-mail: Antar-Y@rmc.ca).

X. Fàbregas is with the Universitat Politecnica de Catalunya (UPC), E-08034 Barcelona, Spain (e-mail: fabregas@tsc.upc.es).

Digital Object Identifier 10.1109/TGRS.2003.817825

medium that presents reflection symmetry. With this assumption, the characteristic polarizations of the medium are orthogonal and linear [3]. In general, it will be considered that they are rotated an angle $\overline{\alpha}$ from vertical–horizontal polarizations as depicted in Fig. 1.

Monostatic radar configuration and homogeneity and reciprocity of the medium are also assumed. Besides this, we consider the following.

1) The polarization basis used for transmitting/receiving is that defined by the characteristic polarizations $\hat{\alpha}$ and $\hat{\beta}$ (in most practical situations, the mean canting angle is zero, and the characteristic polarizations are vertical and horizontal).
2) The wave propagates with a propagation constant $\gamma_{o\alpha}$ or $\gamma_{o\beta}$ depending on the transmitted polarization.
3) The above propagation constants can be expressed as

$$\gamma_{o\alpha} = \gamma_o + \gamma_\alpha \tag{1}$$
$$\gamma_{o\beta} = \gamma_o + \gamma_\beta \tag{2}$$

where $\gamma_o = jk_o$ is the free-space propagation constant, and expressions for γ_α and γ_β as functions of the microphysical characteristics of the rain medium have been provided by different authors [2], [13].

With these premises, fields at points B and C, separated by distance R, can be related as follows:

$$\begin{bmatrix} E_\alpha \\ E_\beta \end{bmatrix}_C = \frac{e^{-\gamma_o R}}{R} \begin{bmatrix} e^{-\gamma_\alpha R} & 0 \\ 0 & e^{-\gamma_\beta R} \end{bmatrix} \begin{bmatrix} E_\alpha \\ E_\beta \end{bmatrix}_B. \tag{3}$$

Now, if backscattering from a single particle at point C is characterized by means of the scattering matrix

$$\begin{bmatrix} S_{\alpha\alpha} & S_{\alpha\beta} \\ S_{\alpha\beta} & S_{\beta\beta} \end{bmatrix} \tag{4}$$

the backscattered field received at point B can be expressed as

$$\begin{aligned} \begin{bmatrix} E_\alpha \\ E_\beta \end{bmatrix}_R &= \frac{e^{-2\gamma_o R}}{R^2} \begin{bmatrix} e^{-\gamma_\alpha R} & 0 \\ 0 & e^{-\gamma_\beta R} \end{bmatrix} \begin{bmatrix} S_{\alpha\alpha} & S_{\alpha\beta} \\ S_{\alpha\beta} & S_{\beta\beta} \end{bmatrix} \\ &\quad \cdot \begin{bmatrix} e^{-\gamma_\alpha R} & 0 \\ 0 & e^{-\gamma_\beta R} \end{bmatrix} \begin{bmatrix} E_\alpha \\ E_\beta \end{bmatrix}_T \\ &= \frac{e^{-2\gamma_o R}}{R^2} \begin{bmatrix} S_{\alpha\alpha} e^{-2\gamma_\alpha R} & S_{\alpha\beta} e^{-(\gamma_\alpha+\gamma_\beta)R} \\ S_{\alpha\beta} e^{-(\gamma_\alpha+\gamma_\beta)R} & S_{\beta\beta} e^{-2\gamma_\beta R} \end{bmatrix} \\ &\quad \cdot \begin{bmatrix} E_\alpha \\ E_\beta \end{bmatrix}_T. \end{aligned} \tag{5}$$

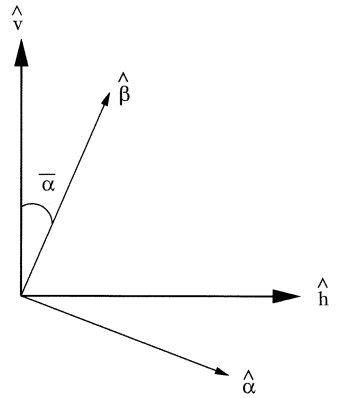

Fig. 1. Characteristic polarizations with respect to H–V polarizations.

Then, the backscatter vector X, which includes scattering and propagation effects, is defined as

$$X = \begin{bmatrix} S_{\alpha\alpha} e^{-2\gamma_\alpha R} \\ \sqrt{2} S_{\alpha\beta} e^{-(\gamma_\alpha+\gamma_\beta)R} \\ S_{\beta\beta} e^{-2\gamma_\beta R} \end{bmatrix}. \tag{6}$$

However, there is general agreement in that second-order moments of backscattered fields should be taken into account to consider scattering characteristics of complex targets like rain. Therefore, the covariance matrix $\mathbf{C}$ [14], defined as the expected value of the Kronecker product of the backscatter vector, presents an appropriate tool to characterize the polarization behavior of complex targets. It can be expressed as in (7), shown at the bottom of the page, where

$$\gamma_{\alpha r} = \mathrm{Re}(\gamma_\alpha) \tag{8}$$
$$\gamma_{\beta r} = \mathrm{Re}(\gamma_\beta) \tag{9}$$

and they indicate one-way specific over-attenuation experienced by the characteristic polarizations with respect to free-space propagation and

$$\Delta\gamma_I = \gamma_{\alpha i} - \gamma_{\beta i} = \mathrm{Im}(\gamma_\alpha) - \mathrm{Im}(\gamma_\beta) \tag{10}$$

is the specific differential phase for one-way propagation as defined in [15]. The quantities $\overline{|S_{\alpha\alpha}|^2}$, $\overline{|S_{\beta\beta}|^2}$, $\overline{|S_{\alpha\beta}|^2}$, and $\overline{S_{\alpha\alpha} S^*_{\beta\beta}}$ are well-known terms that represent, respectively, the copolar power for transmitting/receiving with polarization $\hat{\alpha}$ (channel α), the copolar power for transmitting/receiving with polarization $\hat{\beta}$ (channel β), the cross-polar power for transmitting/receiving with orthogonal polarizations $\hat{\alpha}$ and $\hat{\beta}$ (cross-polar channel), and the copolar correlation between voltages at channels α and β. It is important to realize that the total phase of the copolar correlation term results from

$$\begin{aligned} \mathbf{C} &= \frac{1}{R^4} \cdot \langle X \cdot X^{t*} \rangle \\ &= \frac{1}{R^4} \cdot \begin{bmatrix} \overline{|S_{\alpha\alpha}|^2} e^{-4\gamma_{\alpha r} R} & 0 & \overline{S_{\alpha\alpha} S^*_{\beta\beta}} e^{-2(\gamma_{\alpha r}+\gamma_{\beta r})R} e^{-2j(\gamma_{\alpha i}-\gamma_{\beta i})R} \\ 0 & 2\overline{|S_{\alpha\beta}|^2} e^{-2(\gamma_{\alpha r}+\gamma_{\beta r})R} & 0 \\ \overline{S^*_{\alpha\alpha} S_{\beta\beta}} e^{-2(\gamma_{\alpha r}+\gamma_{\beta r})R} e^{2j(\gamma_{\alpha i}-\gamma_{\beta i})R} & 0 & \overline{|S_{\beta\beta}|^2} e^{-4\gamma_{\beta r} R} \end{bmatrix} \end{aligned} \tag{7}$$

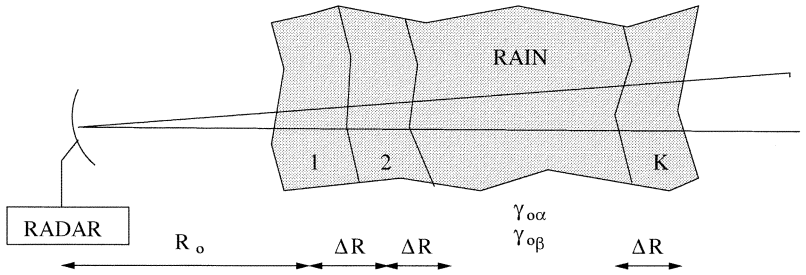

Fig. 2. Radar range gates for propagation parameter estimation.

adding two contributions: $\delta_{\alpha\beta} = \angle(\overline{S_{\alpha\alpha}S^*_{\beta\beta}})$, the copolar backscattering phase, and $2\Delta\gamma_I R$, the differential phase due to propagation in rain. Note that the off-diagonal elements of the covariance matrix that equal zero are due to the reflection symmetry property as was described in [3].

Separating propagation effects from scattering effects the covariance matrix can be rewritten as

$$\mathbf{C} = \frac{1}{R^4}\mathbf{P}\cdot\mathbf{C}_{\alpha\beta}\cdot\mathbf{P}^* \tag{11}$$

where

$$\mathbf{P} = \begin{bmatrix} e^{-2\gamma_{\alpha r}R - j\Delta\gamma_I R} & 0 & 0 \\ 0 & e^{-(\gamma_{\alpha r}+\gamma_{\beta r})R} & 0 \\ 0 & 0 & e^{-2\gamma_{\beta r}R + j\Delta\gamma_I R} \end{bmatrix} \tag{12}$$

$$\mathbf{C}_{\alpha\beta} = \begin{bmatrix} \overline{|S_{\alpha\alpha}|^2} & 0 & \overline{S^*_{\alpha\alpha}S_{\beta\beta}} \\ 0 & 2\overline{|S_{\alpha\beta}|^2} & 0 \\ \overline{S^*_{\alpha\alpha}S_{\beta\beta}} & 0 & \overline{|S_{\beta\beta}|^2} \end{bmatrix}. \tag{13}$$

In a practical radar situation, such as that depicted in Fig. 2, the rain medium is located at a distance R_o away from the radar, and K range samples can be obtained. It is assumed that the spacing of samples in range is equal to the pulse depth ΔR. For a statistical characterization of the data, the polarimetric covariance matrix from each range gate is needed. Based on the previous development and considering that differential propagation effects take place only for distances greater than R_o, where rain is present, the polarimetric covariance matrix that characterizes measurements from the kth range gate can be expressed as

$$\begin{aligned}\mathbf{C}(k) &= \frac{1}{(R_o+k\Delta R)^4}\left\langle X_{\alpha\beta_k}\cdot X^{t*}_{\alpha\beta_k}\right\rangle \\ &= \frac{1}{(R_o+k\Delta R)^4}\mathbf{P}(k)\left\langle X_{\alpha\beta}\cdot X^{t*}_{\alpha\beta}\right\rangle\mathbf{P}^*(k) \\ &= \frac{1}{(R_o+k\Delta R)^4}\mathbf{P}(k)\mathbf{C}_{\alpha\beta}\mathbf{P}^*(k)\end{aligned} \tag{14}$$

with (15) and 16, shown at the bottom of the page. Note that free-space propagation has been assumed for distances less than R_o.

III. Statistical Characterization of Backscattering Matrix Measurements

In this section, statistical characterization of polarimetric backscattering from rain considering uncorrelated signals in time and range will be considered. ML estimators of specific differential phase and attenuation will be derived with these assumptions. Since range gates are centered on the resolution volumes and the spacing of the range gates equals the depth of the resolution volume, assuming uncorrelated data in range is a reasonable approximation. However, data in time is certainly correlated. Effects of time correlation and other measurement errors on the ML estimators to be derived will be considered in Section V.

It is assumed that measurements of the backscattering matrix elements ($S^{kn}_{\alpha\alpha}$, $S^{kn}_{\alpha\beta}$, $S^{kn}_{\beta\beta}$) at any time instant n and from any range gate k can be considered as realizations of a random variable with a multivariate complex Gaussian distribution. Therefore, the probability density function (pdf) that characterizes the statistical behavior of the backscattering matrix n-time sample from the kth range gate is

$$\begin{aligned}f_k\left(S^{kn}_{\alpha\alpha}, S^{kn}_{\alpha\beta}, S^{kn}_{\beta\beta}\right) &= \frac{1}{\pi^3\left|\mathbf{C}(k)\right|} \\ &\cdot\exp\left\{\begin{bmatrix} S^{kn}_{\alpha\alpha} & \sqrt{2}S^{kn}_{\alpha\beta} & S^{kn}_{\beta\beta}\end{bmatrix}^*\mathbf{C}(k)^{-1}\begin{bmatrix} S^{k}_{\alpha\alpha} \\ \sqrt{2}S^{k}_{\alpha\beta} \\ S^{kn}_{\beta\beta}\end{bmatrix}\right\}\end{aligned} \tag{17}$$

where $\mathbf{C}(k)$ represents the covariance matrix corresponding to the kth range gate given in (14), and $|\cdot|$ is used to denote matrix determinant.

If N measurements of each element of the backscattering matrix are obtained from each one of the K range gates, and uncorrelated data in time and range are considered, the pdf that char-

$$\mathbf{P}(k) = \begin{bmatrix} e^{-2\gamma_{\alpha r}k\Delta R - j\Delta\gamma_I k\Delta R} & 0 & 0 \\ 0 & e^{-(\gamma_{\alpha r}+\gamma_{\beta r})k\Delta R} & 0 \\ 0 & 0 & e^{-2\gamma_{\beta r}k\Delta R + j\Delta\gamma_I k\Delta R} \end{bmatrix} \tag{15}$$

$$X_{\alpha\beta_k} = \begin{bmatrix} S^k_{\alpha\alpha} \\ \sqrt{2}S^k_{\alpha\beta} \\ S^k_{\beta\beta}\end{bmatrix} = \mathbf{P}(k)X_{\alpha\beta} = \mathbf{P}(k)\begin{bmatrix} S_{\alpha\alpha} \\ \sqrt{2}S_{\alpha\beta} \\ S_{\beta\beta}\end{bmatrix} \tag{16}$$

acterizes the statistical behavior of the complete dataset may be written as

$$f(\mathbf{S}_\alpha, \mathbf{S}_x, \mathbf{S}_\beta) = \prod_{k=1}^{K} \frac{1}{\pi^{3N} |\mathbf{C}(k)|^N} \cdot \exp\left\{ \sum_{n=1}^{N} \begin{bmatrix} S_{\alpha\alpha}^{kn} & \sqrt{2} S_{\alpha\beta}^{kn} & S_{\beta\beta}^{kn} \end{bmatrix}^* \mathbf{C}(k)^{-1} \begin{bmatrix} S_{\alpha\alpha}^{kn} \\ \sqrt{2} S_{\alpha\beta}^{kn} \\ S_{\beta\beta}^{kn} \end{bmatrix} \right\} \quad (18)$$

where

$$\mathbf{S}_\alpha = \left[S_\alpha^1 \cdots S_\alpha^K \right] \quad (19)$$

$$\mathbf{S}_x = \left[S_x^1 \cdots S_x^K \right] \quad (20)$$

$$\mathbf{S}_\beta = \left[S_\beta^1 \cdots S_\beta^K \right] \quad (21)$$

$$S_\alpha^k = \left[S_{\alpha\alpha}^{k1} \cdots S_{\alpha\alpha}^{kN} \right]^t \quad (22)$$

$$S_x^k = \sqrt{2} \left[S_{\alpha\beta}^{k1} \cdots S_{\alpha\beta}^{kN} \right]^t \quad (23)$$

$$S_\beta^k = \left[S_{\beta\beta}^{k1} \cdots S_{\beta\beta}^{kN} \right]^t. \quad (24)$$

IV. ML Estimates

Though the objective of the present paper is to obtain ML estimators for the differential propagation parameters, ML of covariance matrix $\mathbf{C}_{\alpha\beta}$ is first considered to show that accurate estimation of polarimetric covariance matrix also requires previous estimation of propagation parameters.

In Section III, the statistical behavior of the measured data (backscatter matrix elements) was described. It was found that the data statistics are completely specified by the covariance matrix. The model that will be considered for the covariance matrix was described in Section II. Actually, its elements are functions of the parameters of interest that will be estimated, which are the following:

1) those corresponding to propagation effects, namely

$$\gamma_{\alpha r}, \quad \gamma_{\beta r}, \quad \text{and} \quad \Delta\gamma_I$$

2) those corresponding to backscattering, i.e., the elements of $\mathbf{C}_{\alpha\beta}$, namely

$$\overline{|S_{\alpha\alpha}|^2}, \quad \overline{|S_{\alpha\beta}|^2}, \quad \overline{|S_{\beta\beta}|^2}, \quad \overline{\left|S_{\alpha\alpha} S_{\beta\beta}^*\right|^2}, \quad \text{and} \quad \delta_{\alpha\beta}.$$

Now, to obtain the ML estimators, the log-likelihood function is readily calculated from the pdf specified in (18)

$$\ln f(\mathbf{S}_\alpha, \mathbf{S}_x, \mathbf{S}_\beta) = \sum_{k=1}^{K} \ln \frac{1}{\pi^{3N} |\mathbf{C}(k)|^N} - \sum_{k=1}^{K} \left(N \operatorname{tr}\left(\mathbf{C}(k)^{-1} \cdot \mathbf{S}_{\alpha\beta}^k \right) \right) \quad (25)$$

where $\mathbf{S}_{\alpha\beta}^k$ is the sample covariance matrix corresponding to the kth range gate and can be expressed as in (26), shown at the bottom of the page. Performing the derivatives of the log-likelihood function with respect to the parameters to be estimated, equating to zero and solving the resulting equations, the ML estimators for those parameters are found. Some matrix relations used in the derivations are provided in the Appendix.

A. ML Estimate of $\mathbf{C}_{\alpha\beta}$

To obtain the ML estimate of $\mathbf{C}_{\alpha\beta}$, the gradient with respect to $\mathbf{C}_{\alpha\beta}$ of the log-likelihood function must be calculated and equated to zero, which yields

$$\begin{aligned} \frac{\partial}{\partial \mathbf{C}_{\alpha\beta}} \ln f(\mathbf{S}_\alpha, \mathbf{S}_x, \mathbf{S}_\beta) &= -KN \left(\mathbf{C}_{\alpha\beta}^{-1} \right)^T \\ &\quad + N \left(\mathbf{C}_{\alpha\beta}^{-1} \sum_{k=1}^{K} \mathbf{P}(k)^{-1} \cdot \mathbf{S}_{\alpha\beta}^k \cdot \mathbf{P}(k)^{*-1} \mathbf{C}_{\alpha\beta}^{-1} \right)^T \\ &= 0. \end{aligned} \quad (27)$$

Solution of this equation directly supplies the ML estimate of $\mathbf{C}_{\alpha\beta}$ as

$$\mathbf{C}_{\alpha\beta} = \frac{1}{K} \sum_{k=1}^{K} \mathbf{P}^{-1}(k) \mathbf{S}_{\alpha\beta}^k \mathbf{P}^{*-1}(k). \quad (28)$$

As previously stated, estimation of $\mathbf{C}_{\alpha\beta}$ requires knowledge or previous estimation of the propagation parameters. Their estimation is considered in the next subsections.

B. ML Estimates of Specific Differential Phase $\Delta\gamma_I$

The ML estimate of the specific differential phase can be obtained after differentiating the log-likelihood function with respect to $\Delta\gamma_I$ and equating to zero, which results in the following equation:

$$\operatorname{Im}\left\{ \sum_{k=1}^{K} k e^{(\alpha+\beta)k} \sum_{n=1}^{N} S_{\alpha\alpha}^{kn*} S_{\beta\beta}^{kn} e^{-j\Delta\phi k} e^{+j\delta_{\alpha\beta})} \right\} = 0 \quad (29)$$

where, for notation compactness, the following have been defined:

$$\alpha \doteq 2\gamma_{\alpha r} \Delta R \quad (30)$$

$$\beta \doteq 2\gamma_{\beta r} \Delta R \quad (31)$$

$$\Delta\phi \doteq 2\Delta\gamma_I \Delta R \quad (32)$$

$$\delta_{\alpha\beta} \doteq \angle \left(\overline{S_{\alpha\alpha} S_{\beta\beta}^*} \right). \quad (33)$$

To find the solution of this equation, the copolar backscatter phase $\delta_{\alpha\beta}$ must be estimated in the case that its true value is

$$\mathbf{S}_{\alpha\beta}^k = \frac{1}{N} \begin{bmatrix} \sum_{n=1}^{N} \left| S_{\alpha\alpha}^{kn} \right|^2 & \sqrt{2} \sum_{n=1}^{N} S_{\alpha\alpha}^{kn} S_{\alpha\beta}^{kn*} & \sum_{n=1}^{N} S_{\alpha\alpha}^{kn} S_{\beta\beta}^{kn*} \\ \sqrt{2} \sum_{n=1}^{N} S_{\alpha\beta}^{kn} S_{\alpha\alpha}^{kn*} & 2 \sum_{n=1}^{N} \left| S_{\alpha\beta}^{kn} \right|^2 & \sqrt{2} \sum_{n=1}^{N} S_{\alpha\beta}^{kn} S_{\beta\beta}^{kn*} \\ \sum_{n=1}^{N} S_{\beta\beta}^{kn} S_{\alpha\alpha}^{kn*} & \sqrt{2} \sum_{n=1}^{N} S_{\beta\beta}^{kn} S_{\alpha\beta}^{kn*} & \sum_{n=1}^{N} \left| S_{\beta\beta}^{kn} \right|^2 \end{bmatrix} \quad (26)$$

unknown. Following the same procedure, the ML estimate of $\delta_{\alpha\beta}$ becomes

$$\widehat{\delta_{\alpha\beta}} = -\angle\left(\sum_{k=1}^{K} e^{(\alpha+\beta)k} \sum_{n=1}^{N} S_{\alpha\alpha}^{kn*} S_{\beta\beta}^{kn} e^{-j\widehat{\Delta\phi}k}\right). \quad (34)$$

Now, considering that

$$\sum_{k=1}^{K} e^{(\alpha+\beta)k} \sum_{n=1}^{N} S_{\alpha\alpha}^{kn*} S_{\beta\beta}^{kn} e^{-j\Delta\phi k} = \sum_{k=1}^{K} C_k e^{-j\Delta\phi k} \quad (35)$$

with

$$C_k = e^{(\alpha+\beta)k} \sum_{n=1}^{N} S_{\alpha\alpha}^{kn*} S_{\beta\beta}^{kn} \quad 1 \le k \le K \quad (36)$$

the right-hand side of (35) can be interpreted as the Fourier transform $X_c(e^{j\Delta\phi})$ of the discrete sequence C_k; note that this sequence is a function of the measurements at both copolar channels, and so it is the Fourier transform.

Thus, (29) can be rewritten as

$$\mathrm{Im}\left\{j\, e^{-j\angle[X_c(e^{j\Delta\phi})]} \frac{\partial X_c(e^{j\Delta\phi})}{\partial\Delta\phi}\right\} = 0. \quad (37)$$

Some simple algebraic manipulations lead to the solution of this equation. In fact, the ML estimate of $\Delta\gamma_I$ is

$$\widehat{\Delta\gamma_I} = \frac{1}{2\Delta R} \arg\max_{\Delta\phi} |X_c(e^{j\Delta\phi})| \quad (38)$$

where "$\arg\max_{\Delta\phi}$" should be read as "the value of the argument ($\Delta\phi$) that maximizes." The ML estimate for $\delta_{\alpha\beta}$ is

$$\widehat{\delta_{\alpha\beta}} = -\angle\left(X_c\left(e^{j2\widehat{\Delta\gamma_I}\Delta R}\right)\right). \quad (39)$$

That is, the ML estimate of $\Delta\gamma_I$ is directly proportional to the argument that maximizes the magnitude of the Fourier transform of the range sequence of copolar correlation terms previously corrected for differential attenuation, and the ML estimate of $\delta_{\alpha\beta}$ is the negative of the phase of the previously computed Fourier transform evaluated at $2\widehat{\Delta\gamma_I}\Delta R$.

It is known that sample estimates of the covariance matrix elements corresponding to a particular range gate are unbiased [17]. This fact allows us to conclude that the ML estimates of the specific differential phase and the copolar backscatter phase are asymptotically unbiased and, therefore, their variances asymptotically reach the Cramer–Rao bound. Computation of the Fisher information matrix and its later inversion leads to the following expressions for the Cramer–Rao bounds:

$$\mathrm{var}(\widehat{\Delta\gamma_I}) \ge \frac{1}{2(\Delta R)^2} \frac{3}{KN(K^2-1)} \frac{1-|\rho_{\alpha\beta}|^2}{|\rho_{\alpha\beta}|} \doteq \mathrm{CR}(\widehat{\Delta\gamma_I}) \quad (40)$$

$$\mathrm{var}(\widehat{\delta_{\alpha\beta}}) \ge \frac{1}{2} \frac{(4K^2-1)}{KN(K^2-1)} \frac{1-|\rho_{\alpha\beta}|^2}{|\rho_{\alpha\beta}|} \doteq \mathrm{CR}(\widehat{\delta_{\alpha\beta}}). \quad (41)$$

Figs. 3 and 4 show the square root of the Cramer–Rao bounds normalized to the number of samples per range gate as a function of the path length for different values of the copolar correlation coefficient and different values of range extent of the resolution volume. As an example, it can be observed that the specific differential phase shift can be calculated to an accuracy greater than 0.5 degrees/km for a path length of 2 km and a range extent of the resolution volume of 50 m. In general, the Cramer–Rao bounds decrease as the path length and the copolar correlation increase. The specific differential phase Cramer–Rao bound decreases as the range extent of the resolution volume decreases.

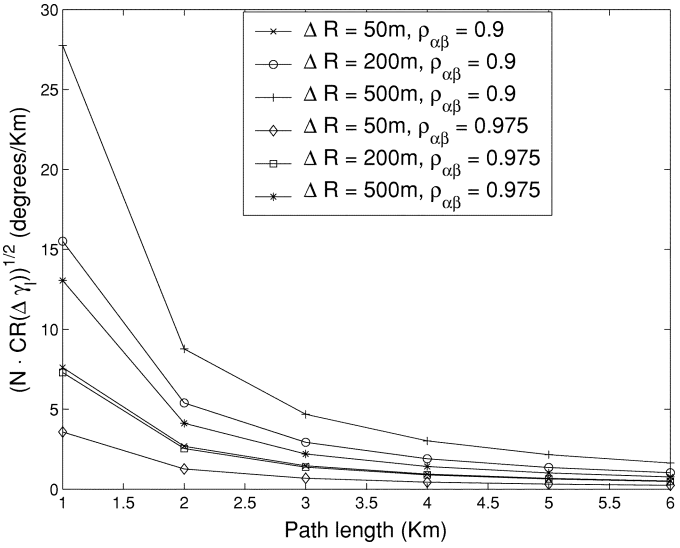

Fig. 3. Square root of the Cramer–Rao bound normalized to the number of samples per range gate of $\Delta\gamma_I$ as a function of the path length for different values of copolar correlation and range extent of the resolution volume.

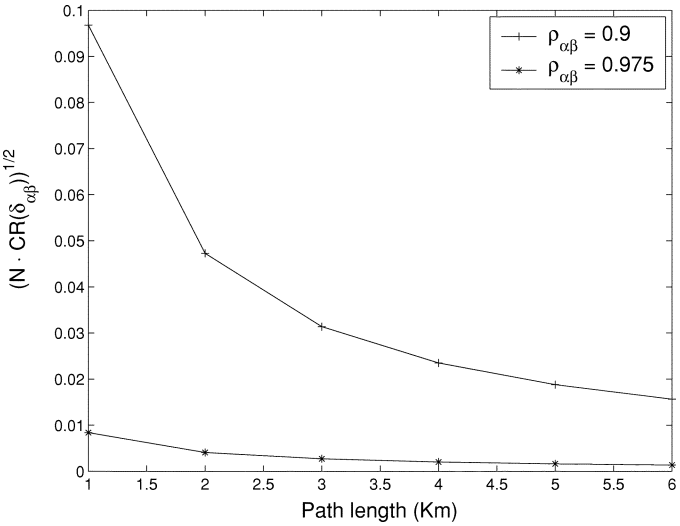

Fig. 4. Square root of the Cramer–Rao bound normalized to the number of samples per range gate of $\delta_{\alpha\beta}$ as a function of the path length for different values of the copolar correlation coefficient.

C. ML Estimates of $\gamma_{\alpha r}$ and $\gamma_{\beta r}$

If the complete available polarimetric dataset is considered to estimate overattenuation of the characteristic polarizations with respect to free-space propagation, then the log-likelihood function given in (25) must be differentiated with respect to $\gamma_{\alpha r}$ and $\gamma_{\beta r}$. This would lead to a set of polynomials in two variables ($\gamma_{\alpha r}$ and $\gamma_{\beta r}$) of high degree (greater than K). Furthermore, the polynomial coefficients are quite involved functions of the elements of $\mathbf{C}_{\alpha\beta}$ and $\Delta\gamma_I$. Thus, finding ML estimates of $\gamma_{\alpha r}$ and $\gamma_{\beta r}$ would require calculating the roots of these polynomials. Previous estimation of $\mathbf{C}_{\alpha\beta}$ elements and $\Delta\gamma_I$ would be necessary. But ML estimation of these parameters also requires

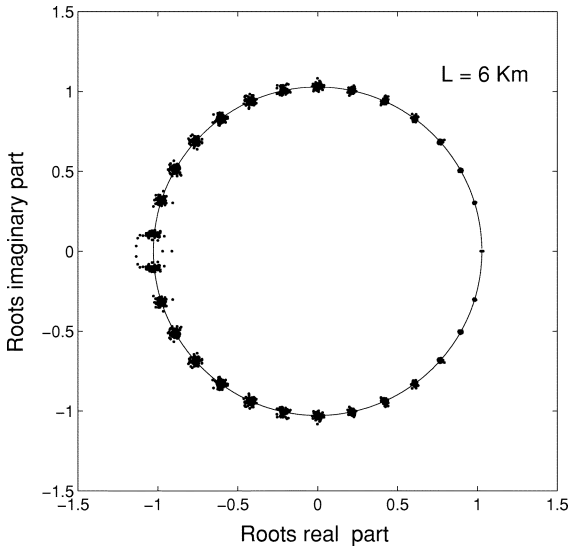

Fig. 5. Roots of 100 polynomials for $N = 64$, $K = 30$, and $\gamma_{\alpha r} = 0.3$ dB/km.

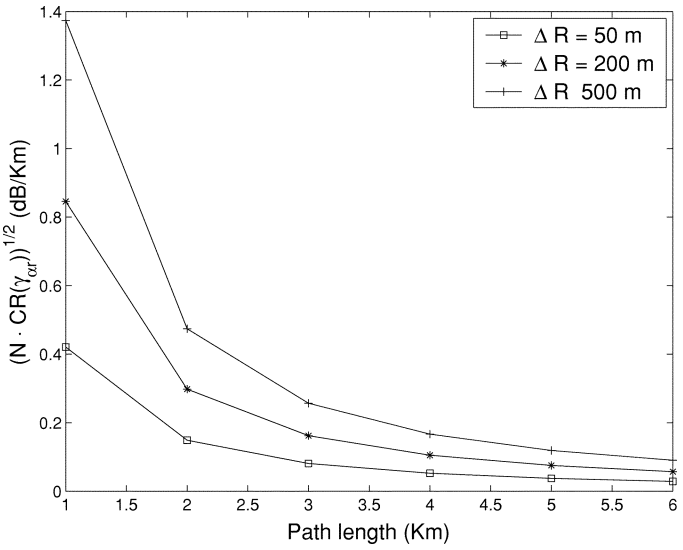

Fig. 6. Square root of the Cramer–Rao bound normalized to the number of samples per range gate of $\gamma_{\alpha r}$ as a function of the path length for different values of range extent of the resolution volume.

estimation of $\gamma_{\alpha r}$ and $\gamma_{\beta r}$. Though numerical methods may be used to get a joint solution for $\mathbf{C}_{\alpha\beta}$, $\Delta\gamma_I$, $\gamma_{\alpha r}$, and $\gamma_{\beta r}$, the results would probably be very sensitive to the initial parameters selection and the numerical method applied. Also, the computational cost of the solution would be very large.

In order to get practically implementable estimates of $\gamma_{\alpha r}$ and $\gamma_{\beta r}$, its ML estimation from data corresponding to only one polarimetric channel was considered. Consequently, estimation of $\gamma_{\alpha r}$ will be based on the sample matrix $\mathbf{S}_\alpha$. Its pdf can be obtained from the pdf given in (18) after integration with respect to $\mathbf{S}_x$ and $\mathbf{S}_\beta$. This results in

$$f(\mathbf{S}_\alpha) = \prod_{k=1}^{K} \frac{1}{\pi^N \left(\overline{|S_{\alpha\alpha}|^2} e^{-2\alpha k}\right)^N} \exp\left\{ \frac{-\sum_{n=1}^{N} \left|S_{\alpha\alpha}^{kn}\right|^2}{\overline{|S_{\alpha\alpha}|^2} e^{-2\alpha k}} \right\}. \tag{42}$$

From this, the log-likelihood function can be calculated as

$$\ln f(\mathbf{S}_\alpha) = \sum_{k=1}^{K} \ln \frac{1}{\pi^N \left(\overline{|S_{\alpha\alpha}|^2} e^{-2\alpha k}\right)^N} - \sum_{k=1}^{K} \frac{\sum_{n=1}^{N} \left|S_{\alpha\alpha}^{kn}\right|^2}{\overline{|S_{\alpha\alpha}|^2} e^{-2\alpha k}}. \tag{43}$$

After computing the gradient of the log-likelihood function with respect to $|S_{\alpha\alpha}|^2$ and α, and equating the result to zero in order to solve for the ML estimates

$$2N \sum_{k=1}^{K} k - \frac{1}{\overline{|S_{\alpha\alpha}|^2}} \sum_{k=1}^{K} 2k e^{2\alpha k} \sum_{n=1}^{N} \left|S_{\alpha\alpha}^{kn}\right|^2 = 0 \tag{44}$$

and

$$\overline{|S_{\alpha\alpha}|^2} = \frac{1}{KN} \sum_{k=1}^{K} \sum_{n=1}^{N} \left|S_{\alpha\alpha}^{kn}\right|^2 e^{2\alpha k} \tag{45}$$

are produced. Substitution of (45) in (44) gives

$$\sum_{k=1}^{K} \sum_{n=1}^{N} (K + 1 - 2k) e^{2\alpha k} \left|S_{\alpha\alpha}^{kn}\right|^2 = 0 \tag{46}$$

which shows that ML estimation of $\gamma_{\alpha r}$ will require to find the zeros of the polynomial given in (46).

In the limiting case of an infinite number of samples from each range gate, taking into account that

$$\frac{1}{N} \sum_{n=1}^{N} \left|S_{\alpha\alpha}^{kn}\right|^2 \to \overline{|S_{\alpha\alpha}|^2} e^{-2\alpha k}$$

and letting $x = e^{2\alpha}$, (46) can be expressed as

$$\sum_{k=1}^{K} (K - (2k-1)) x^k \overline{|S_{\alpha\alpha}|^2} e^{-2\alpha k} = 0. \tag{47}$$

It can be shown that this polynomial possesses a real root at $x = e^{2\alpha}$. Also, it can be shown that the magnitude of all polynomial roots equals $e^{2\alpha}$. Their angles depend only on the number K of resolution range gates considered.

In a real situation, with a finite number of samples, the coefficients of the polynomial given in (46) ($|S_{\alpha\alpha}^{kn}|^2$) would be "around" their expected values ($\overline{|S_{\alpha\alpha}|^2}$), and therefore, its roots will be in the neighborhood of the polynomial's roots given in (47).

Though, the absolute value of all roots of the polynomial given in (46) is close to $e^{2\alpha}$, extensive simulations carried out by the authors for different values of parameters (K, N, α) have shown that the minimum variance corresponds to the real positive root of the polynomial to be solved. As an example, in Fig. 5, the roots corresponding to 100 simulated polynomials with parameters $K = 30$, $N = 64$, and $\gamma_{\alpha r} = 0.3$ dB/km are shown.

The ML estimate of $\gamma_{\alpha r}$ will be expressed as

$$\widehat{\gamma_{\alpha r}} = \frac{1}{4\Delta R} \ln(x_{rp}) \tag{48}$$

where x_{rp} denotes the real positive root of the polynomial. This means that the ML estimate of $\gamma_{\alpha r}$ is directly proportional to the positive real root of the polynomial given in (46).

Moreover, from (46) and (47) it can be concluded that the ML estimator for $\gamma_{\alpha r}$ is asymptotically unbiased and its variance asymptotically achieves the Cramer–Rao bound given by

$$\text{var}(\widehat{\gamma_{\alpha r}}) \geq \frac{1}{(2\Delta R)^2} \frac{3}{4} \frac{1}{NK(4K^2 - 1)} \doteq \text{CR}(\widehat{\gamma_{\alpha r}}). \tag{49}$$

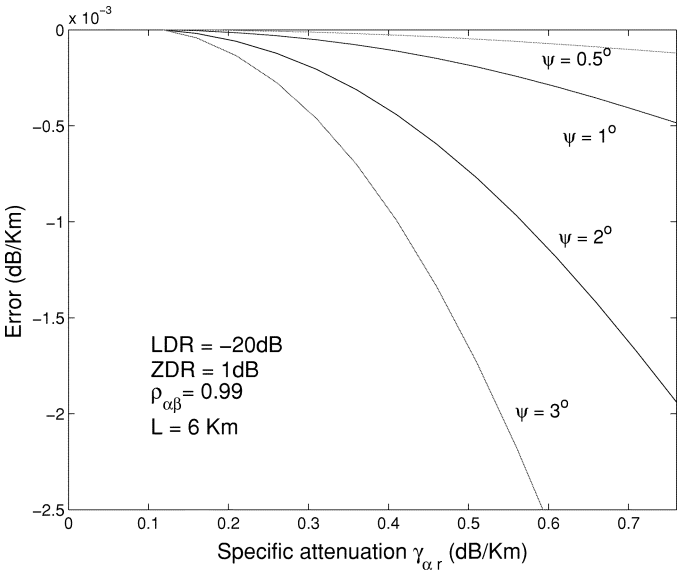

Fig. 7. Sensitivity of specific attenuation estimation for different values of specific attenuation and feed rotation angle ψ.

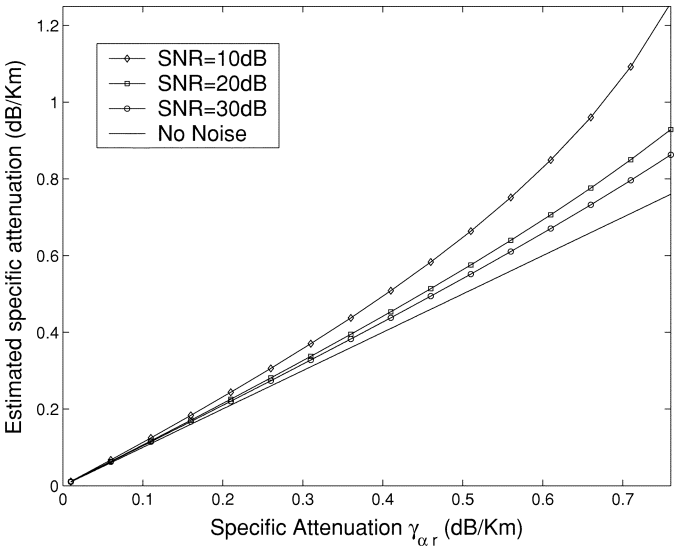

Fig. 8. Sensitivity of specific attenuation estimation for different SNR values.

Fig. 6 shows the square root of the Cramer–Rao bound normalized to the number of samples per range gate as a function of the path length for different values of ΔR. The results suggest that, in theory, for a 2-km path, with a range resolution equal to 50 m, it is possible to obtain $\gamma_{\alpha r}$ with an accuracy close to 0.025 dB/km.

The ML estimate of $\gamma_{\beta r}$ can be obtained following the same procedure though considering the data contained in the $\mathbf{S}_\beta$ matrix.

V. Measurement Considerations

Real radar measurement of hydrometeors polarimetric covariance matrices may be affected by many factors. The purpose of this section is to analyze the sensitivity of the proposed ML estimators for specific attenuation and specific differential phase, to different measurement errors. Actually, the analysis proposed by Doviak *et al.* [16] to study the influence of measurement errors in other estimates of polarimetric variables will be applied to the ML estimators of specific differential phase and attenuation derived. In fact, their sensitivity to feed polarization rotation, drop canting angle along the propagation path, differential phase shifts in the transmitter and receiver, noise at the receiver, and temporal correlation between consecutive samples will be considered.

Having assumed that the linear polarizations used for transmitting/receiving are parallel and perpendicular to the symmetry direction of the medium defined by the mean drop canting angle, effects of feed polarization rotation with respect to the symmetry direction of the medium will be analyzed. Clearly, the effects of erroneous mean drop canting angle determination will be analogous to feed polarization rotation effects.

Defining ψ as the angular displacement (rotation) of the feed polarization with respect to the symmetry direction of the medium, the measured covariance matrix corresponding to the kth range gate $\mathbf{C}^M(k)$ is obtained as

$$\mathbf{C}^M(k) = \mathbf{M} \cdot \mathbf{C}(k) \cdot \mathbf{M}^{t*} \tag{50}$$

where $\mathbf{M}$ is the matrix for polarization basis change defined in [3] with $\theta = \pi/2 + \psi$ and $\phi = \pi/4$.

Straightforward manipulations lead to the following expression for the copolar power from the kth range gate

$$\begin{aligned}\overline{|S_{\alpha\alpha}|^2}^{Mk} = \overline{|S_{\alpha\alpha}|^2} e^{-2\alpha k}\Big(&\sin^4\theta + 2Zdr^{-\frac{1}{2}} e^{2(\alpha-\beta)k}\sin^2\theta \\ &\cdot \cos^2\theta |\rho_{\alpha\beta}| \cos(\delta_{\alpha\beta} - \Delta\phi k) \\ &+ 2\mathrm{Ldr}\sin^2\theta\cos^2\theta e^{(\alpha-\beta)k} \\ &+ \mathrm{Zdr}^{-1} e^{2(\alpha-\beta)k}\cos^4\theta\Big)\end{aligned} \tag{51}$$

where Zdr and Ldr denote the differential reflectivity and the linear depolarization ratio.

Using this expression for $\overline{|S_{\alpha\alpha}|^2}^{Mk}$ in (47), it is found that the expected value of $\gamma_{\alpha r}$ will converge to the solution of

$$\sum_{k=1}^{K} (K + 1 - 2k) x^k \overline{|S_{\alpha\alpha}|^2}^{Mk} = 0. \tag{52}$$

Fig. 7 shows the sensitivity of the estimator for $\gamma_{\alpha r}$ (i.e., the difference between the solution of (52) and the "real" value) to a feed polarization rotation for different values of $\gamma_{\alpha r}$ and different feed rotation angles. High copolar correlation has been assumed. For each value of $\gamma_{\alpha r}$, $\gamma_{\beta r}$, and $\Delta\gamma_I$ have been recalculated using power law fits [18]. Sensitivity to typical values of Zdr and Ldr from precipitation media has been found negligible. Twelve 500-m-long range gates have been considered for calculations. Increasing the number of gates while decreasing the range extent of the resolution volume to maintain the total path length used for estimation would improve the estimation.

Clearly, differential phase shifts introduced in the transmitter and/or receiver will not affect estimation of $\gamma_{\alpha r}$. On the other

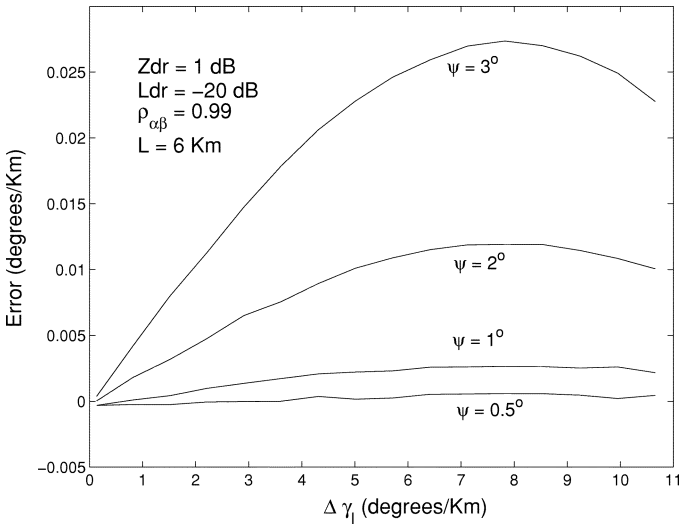

Fig. 9. Sensitivity of specific differential phase estimation for different values of specific differential phase and feed rotation angle ψ.

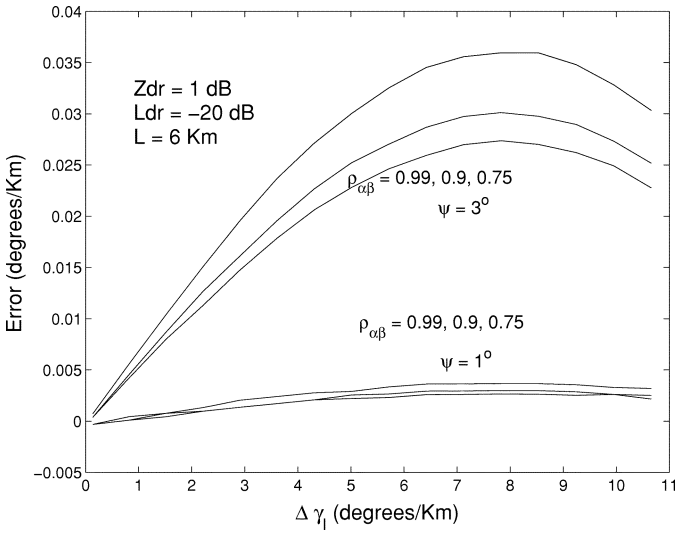

Fig. 10. Sensitivity of specific differential phase estimation to copolar correlation.

hand, temporal decorrelation will not affect the mean value of $\gamma_{\alpha r}$ estimates either, though its standard deviation will increase.

Finally, the effect of system noise is shown in Fig. 8 for different values of the SNR measured with respect to the first range gate. Twelve range gates and ΔR equal to 500 m were considered for estimation. Increasing the number of range gates for the same total path length leads to negligible improvement of the results. Only those range gates whose SNR is greater than zero are considered in the estimation. It can be observed that the proposed estimator is very sensible to noise, so previous estimation of noise power will be required to get accurate estimates.

Now, sensitivity of the estimator for $\Delta\gamma_I$ to feed rotation is analyzed. Estimation of $\Delta\gamma_I$ is based on the Fourier transform of copolar correlation terms. From (50), the copolar correlation term corresponding to the kth range gate as a function of the feed rotation angle is obtained as

$$\begin{aligned}\overline{S^*_{\alpha\alpha}S_{\beta\beta}}^{Mk} = \overline{|S_{\alpha\alpha}|^2}\,\big[&\sin^2\theta\cos^2\theta \\ &\cdot\Big(2\mathrm{Ldr}e^{-(\alpha+\beta)k} - e^{-2\alpha k} - \mathrm{Zdr}e^{-2\beta k}\Big) \\ &- \sin^4\theta\,\mathrm{Zdr}^{\frac{1}{2}}|\rho_{\alpha\beta}|e^{-(\alpha+\beta)k}e^{j\Delta\phi k}e^{-j\delta_{\alpha\beta}} \\ &- \cos^4\theta\,\mathrm{Zdr}^{\frac{1}{2}}|\rho_{\alpha\beta}|e^{-(\alpha+\beta)k}e^{-j\Delta\phi k}e^{j\delta_{\alpha\beta}}\big] \quad (53)\end{aligned}$$

Then, ML estimate of $\Delta\gamma_I$ will be equal to

$$\frac{1}{2\Delta R}\arg\max_{\Delta\phi}\left|X_c(e^{j\Delta\phi})\right| \quad (54)$$

with $X_c(e^{j\Delta\phi})$ being the Fourier transform of the sequence

$$C_k = e^{(\alpha+\beta)k}\overline{S^*_{\alpha\alpha}S_{\beta\beta}}^{Mk}, \qquad 1 \le k \le K. \quad (55)$$

Fig. 9 shows the sensitivity of the estimator for $\Delta\gamma_I$ (the difference between the value of $\Delta\gamma_I$ calculated with (54) and the "real" value) for different values of $\Delta\gamma_I$ and different values of the feed polarization rotation angle. Twelve range gates were considered along the 6-km path. As in the case of specific attenuation estimation, it was found that sensitivity to normal

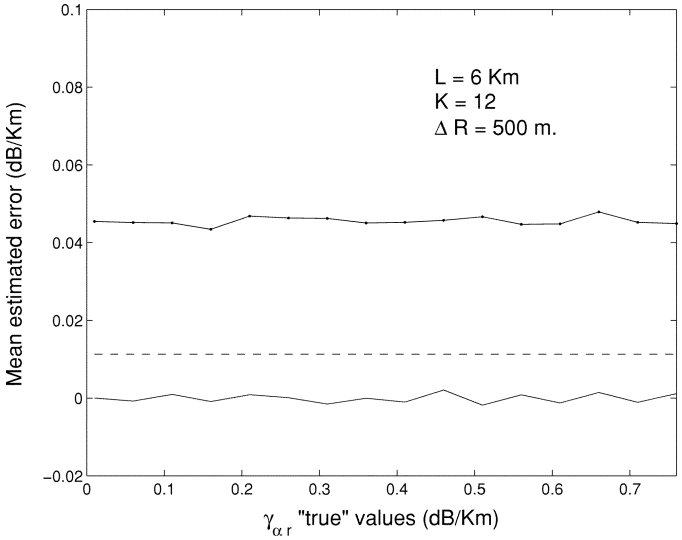

Fig. 11. $\gamma_{\alpha r}$ minus $\gamma_{\alpha r}$ estimated mean value. (Dashed line) Cramer–Rao bound for the standard deviation. (Pointed line) Estimated standard deviation (12 range gates; 6-km path).

variations of Zdr and Ldr in their typical range of values for precipitation media is negligible. More meaningful is the error increase as the copolar correlation decreases. This effect can be observed in Fig. 10 for different values of the copolar correlation coefficient.

Temporal decorrelation between consecutive samples implies a decrease of the copolar correlation coefficient, and therefore its effect, in the case that feed polarization rotation exists, is analogous to the effect observed in Fig. 10. In absence of feed polarization, rotation temporal decorrelation will only imply higher estimator variance.

Finally, as noise at different receiving channels can be considered uncorrelated, its effects on estimation of $\Delta\gamma_I$ will result in higher variances. $\Delta\gamma_I$ estimates will neither be affected

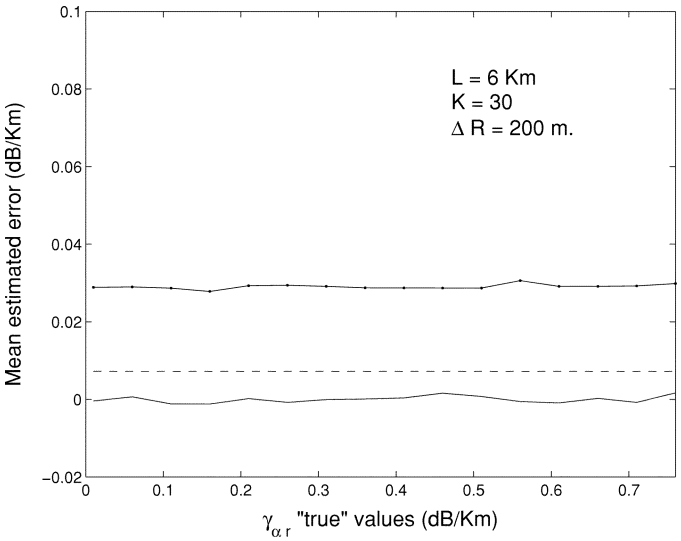

Fig. 12. $\gamma_{\alpha r}$ minus $\gamma_{\alpha r}$ estimated mean value. (Dashed line) Cramer–Rao bound for the standard deviation. (Pointed line) Estimated standard deviation (30 range gates; 6-km path).

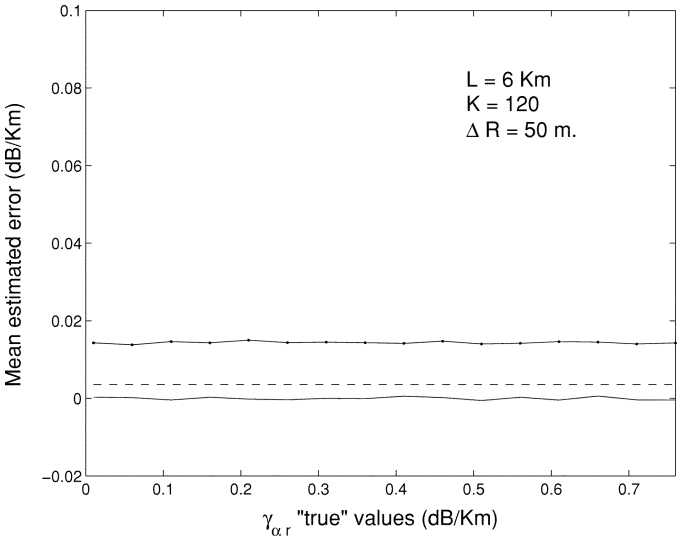

Fig. 13. $\gamma_{\alpha r}$ minus $\gamma_{\alpha r}$ estimated mean value. (Dashed line) Cramer–Rao bound for the standard deviation. (Pointed line) Estimated standard deviation (12 range gates; 6-km path).

by differential phase shifts in the transmitter nor the receiver. These will rather affect estimation of copolar backscattering phase $\delta_{\alpha\beta}$.

VI. Some Results From Simulation

In this section, we present some results based on simulations. Gaussian statistics have been assumed. Ldr $= -30$ dB, Zdr $= 1$ dB, and high copolar correlation $\rho_{\alpha\beta} = 0.975$ have been considered in the simulations. Specific attenuation $\gamma_{\alpha r}$ varying between 0 and 0.8 dB/km has been assumed. Corresponding values of $\gamma_{\beta r}$ and $\Delta\gamma_I$ have been calculated using

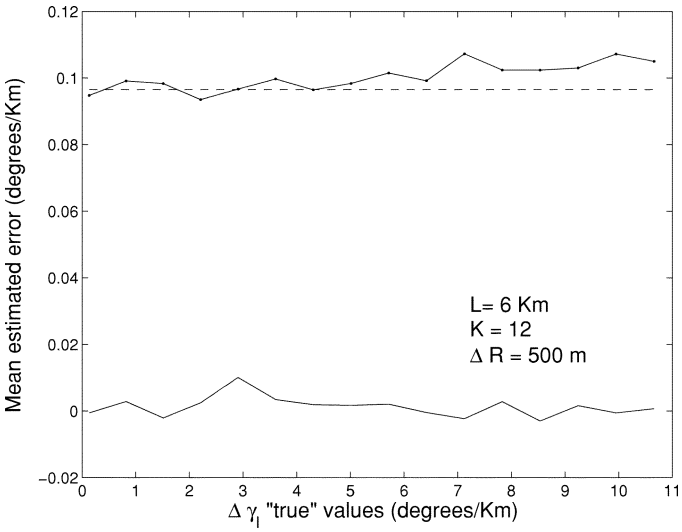

Fig. 14. $\Delta\gamma_I$ minus $\Delta\gamma_I$ estimated mean value. (Dashed line) Cramer–Rao bound for the standard deviation. (Pointed line) Estimated standard deviation (12 range gates; 6-km path).

power law fits [18]. Sixty-four samples from each range gate have been considered.

Figs. 11–13 show the difference in decibels per kilometer between the estimated mean value of the specific attenuation $\gamma_{\alpha r}$ and its "true" value used in the simulations, for a total path length of 6 km; 12, 30, and 120 range gates have been considered. Also, the estimated standard deviation and the Cramer–Rao bound for the standard deviation are shown. Results show a negligible bias of the $\gamma_{\alpha r}$ estimates. It can also be observed that the standard deviation depends only on the number of range gates and the range extent of the resolution volume, and it decreases as the number of range gates increases. Neither the bias nor the standard deviation depend on the $\gamma_{\alpha r}$ value to be estimated; therefore, the relative error (defined as the ratio between the standard deviation to the mean value of the $\gamma_{\alpha r}$ estimate) increases as $\gamma_{\alpha r}$ values approaches zero. In general, estimation of low values of specific attenuation will be more difficult.

Figs. 14–16 show the difference in dB/km between the estimated mean value of the specific differential phase $\Delta\gamma_I$ and its "true" value used in the simulations, for a total path length of 6 km; 12, 30, and 120 range gates have been considered. Estimated standard deviation and the Cramer–Rao bound are also shown. The "apparent" bias of the estimates observed as the number of range gates increases is due only to the finite resolution used to calculate the Fourier transform. The standard deviation is, in this case, very close to the Cramer–Rao bound. In view of the results the, $\Delta\gamma_I$ estimator may be considered as the minimum variance unbiased estimator. Unfortunately, as in the case of $\gamma_{\alpha r}$ estimates, neither the bias, nor the variance of $\Delta\gamma_I$ estimates depend on its value, so, again, estimation of $\Delta\gamma_I$ values close to zero will be more imprecise.

More simulations have been performed with other parameters and taking into consideration noise. It has been observed that for moderate SNR values around 10 dB (measured with respect to

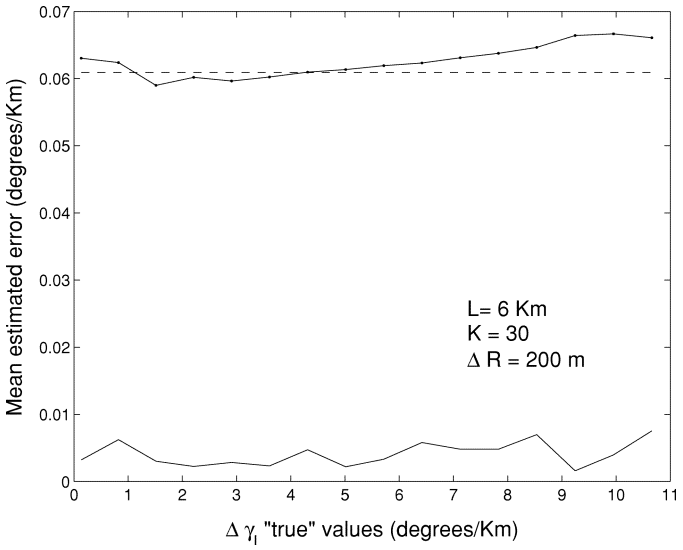

Fig. 15. $\Delta\gamma_I$ minus $\Delta\gamma_I$ estimated mean value. (Dashed line) Cramer–Rao bound for the standard deviation. (Pointed line) Estimated standard deviation (30 range gates; 6-km path).

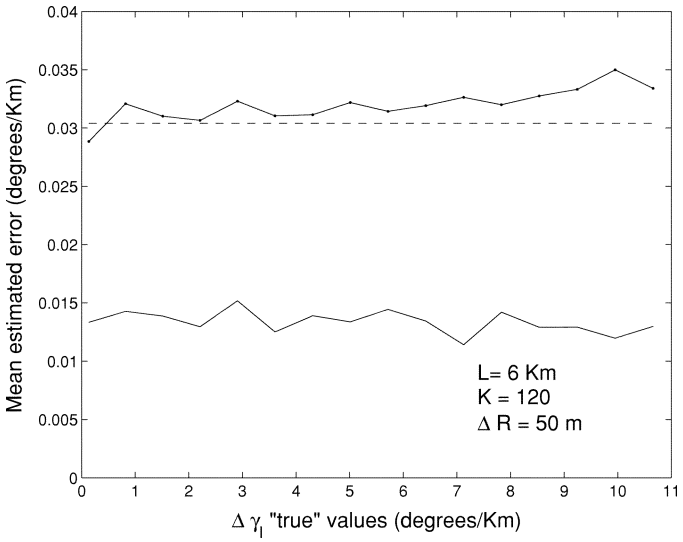

Fig. 16. $\Delta\gamma_I$ minus $\Delta\gamma_I$ estimated mean value. (Dashed line) Cramer–Rao bound for the standard deviation. (Pointed line) Estimated standard deviation (12 range gates; 6-km path).

the first range gate) the performance of the estimators remains good. No bias is observed if the previous estimation of noise is realized though the variance is moderately increased.

Also, it is in order to mention that comparisons between the ML estimator of the specific differential phase proposed and the estimate of these parameter obtained through the least squares fit widely used have been made. For these comparisons, results on the variance of the specific differential phase in [19] have been used. Performance of both methods is in general very good, only for high temporal correlation, and a low number of samples ML estimator performs slightly better.

VII. Conclusion

Maximum-likelihood estimators of differential propagation parameters in rain have been obtained, taking into consideration coherent propagation and reflection symmetry of the medium. Performance of the estimators has been analyzed through simulated data. Results show very good performance for both estimators, especially for the specific differential phase, which from a practical point of view may be considered the minimum variance-unbiased estimator. No noticeable bias has been observed in simulations, and variance has always matched the Cramer–Rao bound. Also, an estimator for the copolar backscattering phase $\delta_{\alpha\beta}$ has been provided. This will allow to separate propagation from scattering contributions. The specific attenuation estimator also showed good performance, unnoticeable bias, and moderate variances that allow quite precise estimation of the parameter. For example, simulations show that for a 6-km path, with a ΔR equal to 200 m, the specific attenuation can be estimated with an accuracy of 0.03 dB/km; if the path is reduced to 2 km, for the same range resolution, the achievable accuracy would be around 0.2 dB/km, which might not be sufficient. For this 2-km path with 50-m range resolution, accuracy would be in 0.1 dB/km. That is, for accurate estimation of specific attenuation, longer paths in homogeneous rain or high range resolution will be required.

A sensitivity analysis to usual measurement errors has been performed. This indicates that small feed polarization rotation has no significant effects on specific attenuation. It may have more important effects on specific differential phase if copolar decorrelation is important. For this reason, a precise estimation of copolar correlation terms is important. Different methods and their performance for measuring copolar correlation terms have been discussed in [20].

With respect to noise, it is clear from the sensitivity analysis and also from simulation results that it must be previously estimated in order to get reliable estimates of specific attenuation. In any case, variances of both parameters—specific attenuation and specific differential phase—will increase.

Finally, temporal decorrelation, in absence of other measurement errors will lead to higher standard deviations too, but it will not have an effect on expected values.

Estimation of propagation parameters is important for propagation effects correction and for separating propagation from scattering effects, and this will also lead to an easier interpretation of the data. Correction of propagation effects in rain requires the capability of estimating differential propagation parameters in all range gates between the radar and the target (may be a remote rain cell). This is not possible in many real situations where data from the first range gates may be contaminated by clutter. Still, in these cases, it may be of interest to determine specific attenuation and/or specific differential phase for rainfall estimation in remote areas. The proposed estimators of differential propagation parameters can be used for any set of K consecutive range gates, even if they are not located at the beginning of the path.

$$\mathbf{C}(k) = \mathbf{P}(k) \cdot \mathbf{C}_{\alpha\beta} \cdot \mathbf{P}(k)^*$$
$$\mathbf{C}(k)^{-1} = \mathbf{P}(k)^{*-1} \cdot \mathbf{C}_{\alpha\beta}^{-1} \cdot \mathbf{P}(k)^{-1}$$

$$|\mathbf{C}(k)| = |\mathbf{P}(k)| \cdot |\mathbf{C}_{\alpha\beta}| \cdot |\mathbf{P}(k)^*| = |\mathbf{P}(k)|^2 \cdot |\mathbf{C}_{\alpha\beta}|$$

$$\mathrm{tr}\left(\mathbf{C}(k)^{-1}\mathbf{S}_{\alpha\beta}^k\right) = \mathrm{tr}\left(\mathbf{P}(k)^{*-1} \cdot \mathbf{C}_{\alpha\beta}^{-1} \cdot \mathbf{P}(k)^{-1} \cdot \mathbf{S}_{\alpha\beta}^k\right) = \mathrm{tr}\left(\mathbf{C}_{\alpha\beta}^{-1} \cdot \mathbf{P}(k)^{-1} \cdot \mathbf{S}_{\alpha\beta}^k \cdot \mathbf{P}(k)^{*-1}\right)$$

$$\mathbf{C}(k)^{-1} = \frac{1}{|\mathbf{C}_{\alpha\beta}|}\mathbf{P}(k)^{*-1}\begin{bmatrix} \overline{|S_{\alpha\beta}|^2}\,\overline{|S_{\beta\beta}|^2} & 0 & -\overline{|S_{\alpha\beta}|^2}\,\overline{S_{\alpha\alpha}S_{\beta\beta}^*} \\ 0 & \overline{|S_{\alpha\alpha}|^2}\,\overline{|S_{\beta\beta}|^2} - \left|\overline{S_{\alpha\alpha}S_{\beta\beta}^*}\right|^2 & 0 \\ -\overline{|S_{\alpha\beta}|^2}\,\overline{S_{\alpha\alpha}^*S_{\beta\beta}} & 0 & \overline{|S_{\alpha\alpha}|^2}\,\overline{|S_{\alpha\beta}|^2} \end{bmatrix}\mathbf{P}(k)^{-1}$$

To conclude, it is of importance to note that the proposed estimators are independent of the microphysical characteristics of the medium as far as it presents reflection symmetry and coherent propagation can be assumed. Therefore, they provide a new way for measuring and validating microphysical characteristics of the medium such as size or orientation distribution.

APPENDIX
SOME MATRIX RELATIONS

See the equations at the top of the page.

ACKNOWLEDGMENT

The authors thank C. Garcia del Cueto for helping in preparing the manuscript.

REFERENCES

[1] T. Oguchi, "Electromagnetic wave propagation and scattering in rain and other hydrometeors," *Proc. IEEE*, vol. 71, pp. 1029–1077, 1983.
[2] R. L. Olsen, "A review of theories of coherent radio wave propagation through precipitation media of randomly oriented scatterers and the role of multiple scattering," *Radio Sci.*, vol. 17, pp. 913–928, 1982.
[3] V. Santalla, Y. M. M. Antar, and A. Pino, "Polarimetric radar covariance matrix algorithms and applications to meteorological targets," *IEEE Trans.Geosci. Remote Sensing*, vol. 37, pp. 1128–1138, Mar. 1999.
[4] J. Hubbert, V. Chandrasekar, V. N. Bringi, and P. Meischner, "Processing and interpretation of coherent dual-polarized radar measurements," *J. Atmos. Ocean. Technol.*, vol. 10, pp. 155–164, 1993.
[5] J. Hubbert and V. N. Bringi, "An iterative filtering technique for the analysis of copolar differential phase and dual-frequency radar measurements," *J. Atmos. Ocean. Technol.*, vol. 12, pp. 643–648, 1995.
[6] N. Balakrishnan and D. S. Zrnic, "Estimation of rain and hail rates in mixed phase precipitation," *J. Atmos. Sci.*, vol. 47, pp. 565–583, 1990.
[7] E. Gorgucci, G. Scarchilli, and V. Chandrasekar, "Specific differential phase shift estimation in the presence of nonuniform rainfall medium along the path," *J. Atmos. Ocean. Technol.*, vol. 16, pp. 1690–1697, 1999.
[8] V. N. Bringi, V. Chandrasekar, N. Balakrishnan, and D.S. Zrinic, "An examination of propagation effects in rainfall on radar measurements at microwave frequencies," *J. Atmos. Ocean. Technol.*, vol. 7, pp. 829–840, 1990.
[9] K. Aydin, Y. Zhao, and T. A. Seliga, "Rain induced attenuation effects on C-band dual-polarization meteorological radars," *IEEE Trans. Geosci. Remote Sensing*, vol. 27, pp. 57–66, Jan. 1989.
[10] E. Gorgucci, G. Scarchilli, and V. Chandrasekar, "Error structure of radar rainfall measurements at C-band frequencies with dual-polarization algorithm for attenuation correction," *J. Geophys. Res.*, vol. 101, pp. 26 461–26 471, 1996.
[11] A. Ryzhkov and D. S. Zrinic, "Precipitation and attenuation measurements at 10 cm wavelength," *J. Appl. Meteorol.*, vol. 34, pp. 2121–2134, 1995.
[12] E. Gorgucci, G. Scarchilli, V. Chandrasekar, P. F. Meischner, and M. Hagen, "Intercomparison of techniques to correct for attenuation of C-band weather radar signals," *J. Appl. Meteorol.*, vol. 37, pp. 845–853, 1998.
[13] T. Oguchi, "Scattering properties of pruppacher and pitter from raindrops and cross polarization due to rain: Calculation at 11, 13, 19.3 and 34.8 Ghz.," *Radio Sci.*, vol. 12, pp. 41–51, 1977.
[14] K. Tragl, "Polarimetric radar backscattering from reciprocal random targets," *IEEE Trans.Geosci. Remote Sensing*, vol. 28, pp. 856–864, Sept. 1990.
[15] R. J. Doviak and D. S. Zrnic, *Doppler Radar and Weather Observations*, 2nd ed. Orlando, FL: Academic, 1993.
[16] R. J. Doviak, V. N. Bringi, A. Ryzhkov, A. Zahrai, and D. S. Zrnic, "Considerations for polarimetric upgrades to operational WSR-88D radars," *J. Atmos. Ocean. Technol.*, vol. 17, pp. 257–278, 2000.
[17] R. J. A. Tough, D. Blacknell, and S. Quegan, "A statistical description of polarimetric and interferometric synthetic aperture radar data," in *Proc. R. Soc. London. A.*, vol. 449, 1995, pp. 567–589.
[18] V. N. Bringi and V. Chandrasekar, *Polarimetric Doppler Weather Radar. Principles and Applications*, 1st ed. Cambridge, U.K.: Cambridge Univ. Press, 2001.
[19] A. V. Ryzhkov and D. S. Zrnic, "Polarimetric rainfall estimation in the presence of anomalous propagation," *J. Atmos. Ocean. Technol.*, vol. 15, pp. 1320–1330, 1998.
[20] V. Santalla and Y. M. M. Antar, "A comparison between different polarimetric measurement schemes," *IEEE Trans.Geosci. Remote Sensing*, vol. 40, pp. 1007–1017, May 2002.

V. Santalla del Rio (M'90) was born in Monterroso, Lugo, Spain, in 1968. She received the M.S. degree in 1990 and the Ph.D. degree in 1996, both in telecommunication engineering from the University of Vigo, Vigo, Spain.

She has been with the Department of Teoría de la Señal y Comunicaciones, University of Vigo, since 1990, and in 1998, she became an Associate Professor. During 1994 and 1995, she spent time at the Department of Electrical and Computer Engineering, the Royal Military College, Kingston, ON, Canada, as a Visiting Researcher. Her research interests include analysis and estimation of polarimetric radar data, weather radar, volume and rough surfaces scattering modeling, scattering statistics, and propagation modeling in natural and urban terrain.

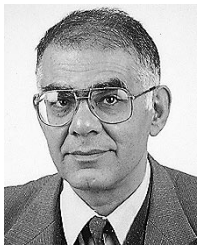

Yahia M. M. Antar (S'73–M'76–SM'85–F'00) was born in Meit Temmama, Egypt, on November 18, 1946. He received the B.Sc. degree (with honors) from Alexandria University, Alexandria, Egypt, in 1966, and the M.Sc. and Ph.D. degrees from the University of Manitoba, Winnipeg, MB, Canada, in 1971 and 1975, respectively, all in electrical engineering.

In 1966, he joined the Faculty of Engineering, Alexandria University, where he was involved in teaching and research. At the University of Manitoba, he held a University Fellowship and NRC Postgraduate and Postdoctoral Fellowships. From 1976 to 1977, he was with the Faculty of Engineering, University of Regina, Regina, SK, Canada. In June 1977, he was awarded a Visiting Fellowship from the Government of Canada to work at the Communications Research Centre, Department of Communications, Shirley's Bay, Ottawa, ON, Canada, where he was involved in research and development of satellite technology with the Space Electronics Group. In May 1979, he joined the Division of Electrical Engineering, National Research Council of Canada, Ottawa, where he worked on polarization radar applications in remote sensing of precipitation, radio wave propagation, electromagnetic scattering, and radar cross section investigations. In November 1987, he joined the staff of the Department of Electrical and Computer Engineering, Royal Military College of Canada, Kingston, ON, where he is now Professor of electrical and computer engineering. His current research interests include polarization studies, integrated antennas, and microwave and millimeterwave circuits. He has authored or coauthored over 100 journal papers on these topics and has supervised or cosupervised over 45 Ph.D. and M.Sc. theses at the Royal Military College and Queen's University, Kingston, of which three have received the Governor General Gold Medal. He is currently the Chairman of the Canadian National Commission (CNC, URSI), holds adjunct appointment at the University of Manitoba, and has a cross appointment at Queen's University.

Dr. Antar is an Associate Editor of the *IEEE Antennas and Propagation Magazine* and Associate Editor of the IEEE TRANSACTIONS ON ANTENNAS AND PROPAGATION. In 2003, he received the RMC Excellence in Research Prize. He became the holder of a Canada Research Chair (CRC) in Electromagnetic Engineering in May 2002.

Xavier Fabregas (M'90) received the B.S. degree in physics from Barcelona University, Barcelona, Spain, in 1988, and the Ph.D. degree in applied sciences from the Technical University of Catalonia (UPC), Barcelona, in 1995.

Since 1996, he has been an Associate Professor with UPC. In 2001, he spent an eight-month sabbatical period at the HR Institute of the German Aerospace Agency (DLR), Oberpfaffenhofen, Germany. His current research interests include polarimetric retrieval algorithms, polarimetric calibration, polarimetric SAR classification, and polarimetric weather radar analysis.